

An Adjustable and Reversible Data Hiding Method Based on Multiple-base Notational System without Location Map

Chin-Feng Lee

Department of Information Management
Chaoyang University of Technology
168, Jifeng E.Rd., Wufeng District, Taichung, 41349, Taiwan
lcf@cyut.edu.tw

Chin-Chen Chang*

Department of Information Engineering and Computer Science
Feng Chia University
No. 100, Wen-Hwa Rd., Taichung, 40724, Taiwan
Department of Computer Science and Information Engineering
Asia University
No. 500, Lioufeng Rd., Wufeng, Taichung, 41354, Taiwan
* Corresponding author: alan3c@gmail.com

Pei-Yan Pai

Department of Compute Science
National Tsing-Hua University
No. 101, Sec. 2, Kuang-Fu Rd., Hsinchu, 30013, Taiwan
d938338@oz.nthu.edu.tw

Chia-Ming Liu

Department of Information Engineering and Computer Science
Feng Chia University
No. 100, Wen-Hwa Rd., Taichung, 40724, Taiwan
sam30525sam@gmail.com

Received March, 2013; revised June, 2013

ABSTRACT. *The reversible image hiding method is one data hiding technique for protecting secret data or copyright. The reversible image hiding method can completely reconstruct the cover image from the stego-image after the embedded secret data are completely extracted. However, many proposed reversible image hiding methods require a location map to restore the cover images. Although the location map can be compressed by a lossless compression algorithm, it will decrease the embedding capacity and increase the computational cost. This paper presents a new type of adjustment reversible image hiding method without a location map. The proposed method applies the multiple-base notational system to embed the secret data into a cover image with minimal distortion and provides several advantages: (1) the location map is not required; (2) the embedding capacity can be adjusted according to the user's practical applications; (3) a high embedding capacity with pleasing visual image quality, especially the smooth images, is achieved. Furthermore, the experimental results demonstrate that the proposed method achieves a higher embedding capacity and satisfactory visual image quality.*

Keywords: Reversible image hiding; Median edge detection predictor; Embedding capacity; Modulus operator

1. **Introduction.** Because information has been digitized due to the rapid development of the Internet, people often transmit data through the Internet for convenience. However, hackers can easily steal, duplicate, or revise such data. As the result, it is important to determine how to protect secret data. Various data hiding techniques have been developed [10].

The image hiding method is used to conceal secret data into the host image, also called a cover image, by modifying the original cover image pixels without introducing perceptual changes. After the secret data are embedded, the cover image is modified to generate a new image, which is called a stego-image. The human eye cannot distinguish the difference between the stego-image and the cover image. Two important requirements of image hiding method are preserving the quality of the stego-image and providing a higher embedding capacity. However, this presents a trade-off problem [7]. It is difficult to provide a high quality stego-image while increasing the embedding capacity at the same time.

The image hiding method can be classified into two categories: reversible and non-reversible. The least significant bit (LSB) replacement method [17] is a well-known non-reversible image hiding method, which replaces some LSBs of cover pixels to embed secret data. Zhang et al. [19] proposed a new data hiding method based on exploiting the modification direction (EMD). In the EMD method, the secret data are transformed into a secret digit in a $(2n + 1)$ -ary notational system. Then, a group consisting of n pixels is used to carry one secret digit. The maximum embedding rate of the EMD method is about 1.16 bits per pixel (bpp) when $n = 2$. Lee et al. [7] presented an improved EMD method based on pixel segmentation to increase the embedding rate. In Lee et al.'s method, each pixel-pair is segmented into two parts: one is applied to embed the secret data, and the other is used as an indicator for extracting the secret data. Lee et al.'s method can provide an embedding rate of more than 1.7 times that of the EMD method. In general, the non-reversible image hiding method can provide higher embedding rates. However, the main drawback is that the cover image cannot be completely reconstructed from the stego-image when the secret data are extracted. In some applications, such as medical, military, and law enforcement applications, restoration of cover image without any distortion is essential [9].

In the reversible image hiding method, the original cover image can be completely restored after the secret data have been extracted. Numerous reversible image hiding methods have been proposed with limiting embedding capacity in the past decade [1, 2, 3, 4]. Tian [13] presented a new reversible data hiding method using difference expansion. The cover pixels are partitioned into several non-overlapping pixel-pairs, each of which comprises two neighboring pixels, and the difference of a pixel-pair is expanded to embed a secret data bit. However, some expanded pixel-pairs may be subjected to the overflow/underflow problem when the secret data are embedded. Therefore, a location map is required to indicate whether each pixel-pair is embeddable. Furthermore, the maximal embedding rate of Tian's method is approximately 0.5 bpp [13]. It does not have enough extra spaces to carry the secret data if the scheme directly embeds the location map into the cover image. Hence, an efficient lossless compression technology needs to be used in order to reduce the size of the location map so that more space can be used for secret data. Unfortunately, the compression rate of the location map is lower when the cover image is complex. Moreover, the computation cost is increased for the embedding process due to lossless compression of the location map.

Ni et al. [11] introduced a high image quality reversible data hiding method based on histogram shifting. This method first finds the maximum peak and zero or minimum point from the histogram of the cover image. The secret data are embedded by shifting the pixel bin's location between the maximum peak and zero or the minimum point. Although Ni et al.'s method can produce a higher of peak signal-to-noise rate (PSNR) at 48 dB, the embedding capacity of Ni et al.'s method is limited by the number of peak bins. In order to completely reconstruct the cover image, Ni et al.'s method needs to keep the overhead information including the values for the maximum peak, zero or minimum point, and some location information for those pixels which may incur overflow/underflow after the secret data have been embedded.

In recent years, many reversible image hiding methods [9, 15, 16, 19] have been proposed to increase the embedding capacity and improve the visual image quality of Tian's scheme or Ni et al.'s scheme. Lin et al. [9] presented a new histogram-based method using a multilevel hiding strategy to obtain high embedding capacity and reduce image distortion. In Lin et al.'s method, the secret data are embedded using histogram modification of different images for each block. Tsai et al. [15] proposed a reversible data hiding method that combines predictive coding and histogram shifting methods. Their method first divides the cover image into several blocks. Next, predictive code is used to predict the center pixel (also called the basic pixel) from its neighboring pixels in each block to generate the residual image. Finally, the secret data are embedded using histogram modification. Tsai et al.'s method needs a large space to record the overhead information due to the large number of peaks and zero bins.

In order to reconstruct the original cover image from the stego-image, most reversible image hiding methods exploit difference expansion or histogram shifting techniques, which require extra information (i.e. location map or overhead information) for data extraction and image restoration. The embedding capacity (also called payload) consists of the extra information and secret data. Obviously, the extra information will reduce the embedding capacity for confidential information; the actual embedding capacity of secret data for a cover image is also called the pure payload. Tseng et al. [16] presented a prediction-based reversible data hiding method for restoring the original cover image from stego-image without location map. The receiver can completely extract the secret data and recover the original cover image from the stego-image according to the difference values between the predictive pixels and the stego-pixels. However, the embedding capacity of Tseng et al.'s method is limited by the number of difference values.

In this paper, a new reversible image hiding method based on a multiple-base notational system without location map is proposed. The proposed method is composed of pre-processing, embedding, and extracting and restoring procedures. The pre-processing procedure modifies some cover pixels which may incur overflow/underflow, and the original cover image is transformed into a modified cover image. Next, the secret data are embedded into a modified cover image using a multiple-base notation system in the embedding procedure. In the extracting and restoring procedure, the secret data are extracted, and the original cover image is restored completely from the stego-image without a location map. The experimental results indicate that the proposed method achieves high embedding capacity and good visual image quality. Furthermore, in the proposed method, the embedding capacity can be adjusted according to the user's particular requirement.

The rest of this paper is organized as follows. In Section 2, the median edge detection (MED) predictor is reviewed. Then, in Section 3, the proposed method including pre-processing, embedding, and extracting and restoring procedures is introduced. In Section 4, we compare the embedding capacity and stego-image quality of the proposed method and other related methods. Finally, conclusions are provided in Section 5.

2. Median Edge Detection (MED) Predictor. The median edge detection (MED) predictor [18], or LOCO-I predictor, is adopted in JPEG-LS technology to predict the pixel value. The MED predictor uses a predictive scheme works on the three nearest neighbors (upper, left, and upper-left) denoted as a , b , and c , respectively, to estimate the value of current pixel x , as shown in FIGURE 1. The predictive value of x is denoted as x' and can be computed as follows:

$$x' = \begin{cases} \min(a, b), & \text{if } c \geq \max(a, b), \\ \max(a, b), & \text{if } c \leq \min(a, b), \\ a + b - c, & \text{otherwise,} \end{cases} \quad (1)$$

where $\min(a, b)$ and $\max(a, b)$ represent the smaller and larger function in calculating a and b , respectively. The three simple predictors are selected according to the following conditions:

- (1) If a vertical edge exists at left of the current pixel, the predictor selects b as the value of the prediction (i.e. $x' = b$).
- (2) If a horizontal edge is above the current pixel, then a is chosen as the predictive value.
- (3) The current pixel is located at the smooth area, so no edge is detected.

The predictor estimates the predictive value as $a + bc$. The prediction error e is given by Equation (2):

$$e = x - x'. \quad (2)$$

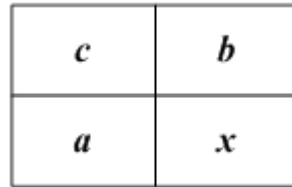


FIGURE 1. MED predictor template

The median edge detection (MED) predictor estimates the gray level of a pixel by detecting whether there is an edge passing through the pixel. MED has the difference e , and the entropy rates of the prediction error images decrease more than those of the original images. In fact, most entropy rates of the error images are close to half those of the original images. This de-correlation of images produces more data redundancies in the prediction error images and creates more quantities of data to be concealed within images.

3. Proposed Method. The proposed method consists of three procedures: pre-processing, embedding, and extracting and restoring. In the pre-processing procedure, some cover pixels are modified to avoid the overflow/underflow problem when the secret data are embedded. The secret data are embedded using a multiple-base notational system in the embedding procedure. In the extracting and restoring procedure, the secret data are extracted exactly, and the original image can be recovered completely. FIGURE 2 shows the flowchart of the proposed method.

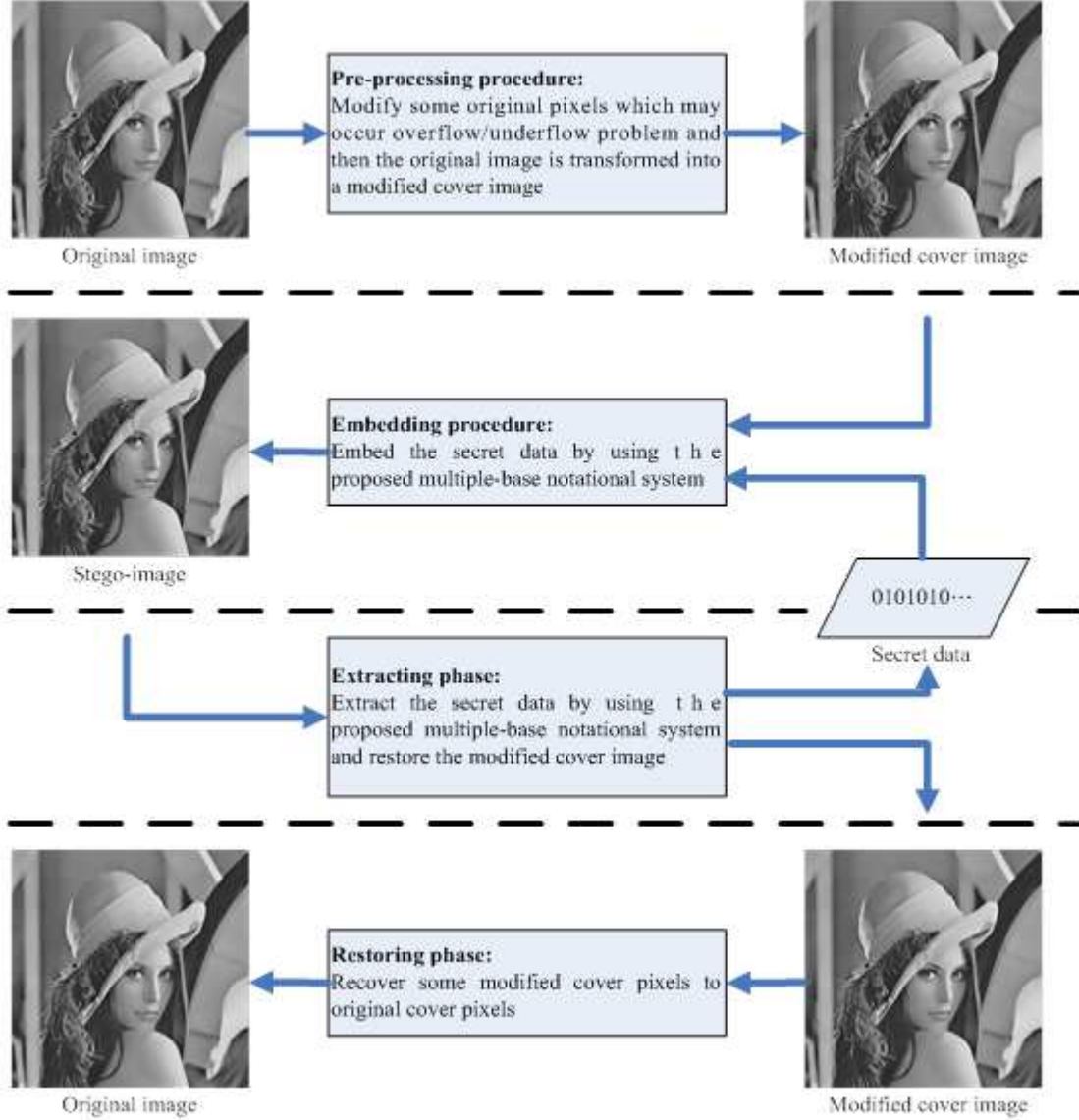


FIGURE 2. The flowchart of the proposed method

3.1. Pre-processing procedure. Before presenting the proposed method, some notations are defined as follows. The cover image I is an 8-bit gray-level image of size is $M \times N$. The $I(x, y)$ represents a pixel located at coordinate (x, y) in the cover image, where $0 \leq x \leq M - 1$ and $0 \leq y \leq N - 1$. To address the overflow/underflow problem, except for the original pixels in the first row and first column, the original pixel belonging to $[0, T_2]$ is converted into T_2 . Similarly, if the original pixel belongs to $[255 - T_2, 255]$, the pixel value is modified to the value of $(255 - T_2)$, and T_2 can be calculated as follows.

$$T_2 = \lfloor (S_{\max} + 1)/2 \rfloor \times b_1, \text{ and } T_1 = \lfloor (b_1 - 1)/2 \rfloor, \quad (3)$$

where T_1 and T_2 are two constants, b_1 is a prior selected base, and S_{\max} is a selected value from $[1, b_1 - 1]$. To recover the modified cover pixel to the original pixel, a k -LSB bit-string, where $k = \lceil \log_2(T_2 + 1) \rceil$, is used to indicate the original k -LSBs of each pixel within the range of values $[0, T_2]$ or $[255 - T_2, 255]$. Accordingly, each original pixel value in $[0, T_2]$ is transformed into k -bit codes " $o_1o_2\dots o_k$ " (i.e. if $T_2 = 12$, then $k = 4$, so that the values 0, 1, ..., 12 are presented as four-bit strings "0000," "0001," ..., "1100," respectively.) Similarly, each original pixel value within $[255 - T_2, 255]$ is encoded as

243 = “0011”, 244 = “0100”, ..., and 255 = “1111” when $k = 4$ and $T_2 = 12$. The original image is scanned by raster-scan order. Except for those pixels located in first row and first column, if the to-be-processed pixel value originally belongs to $[0, T_2]$, then the code “ $o_1o_2\dots o_k$ ” for that pixel is appended to the end of left-sequence bit-stream O_l such as $O_l = O_l \parallel “o_1o_2\dots o_k”$ and the original pixel value is modified to T_2 , where ‘ \parallel ’ is a concatenated operator. Similarly, if the original pixel value is within $[255 - T_2, 255]$, then its code “ $o_1o_2\dots o_k$ ” is appended to the front of right-sequence bit-stream O_r such that $O_r = “o_1o_2\dots o_k” \parallel O_r$, and the original pixel value is changed to $255 - T_2$. Finally, the left and right sequences are concatenated as a bit-stream as the overhead information O , which is $O_l \parallel O_r$ and is further concatenated with the secret data S as payload $P = O \parallel S$ into the modified cover image.

After the pre-processing procedure, the original image is transformed into a modified cover image I' . The following example demonstrates how the pre-processing procedure works to produce a corresponding modified cover image when an original image is given.

Example 1. FIGURE 3(a) displays a 4×4 cover image. The pixels located in the first row or first column are marked in green and remain unchanged. Let b_1 be 5 and S_{\max} be 3. $T_1 = \lfloor (5-1)/2 \rfloor = 2$ and $T_2 = \lfloor (3+1)/2 \rfloor \times 5 + 2 = 12$ are calculated by Equation (3) so that $k = \lceil \log_2(12+1) \rceil = 4$. Since $I(3, 1) = 6 = “0110,”$ $I(1, 2) = 253 = “1101,”$ $I(2, 2) = 12 = “1100,”$ and $I(2, 3) = 245 = “0101”$ belong to $[0, 12]$ or $[243, 255]$, those pixels are changed to $I'(3, 1) = 12$, $I'(1, 2) = 243$, $I'(2, 2) = 12$, and $I'(2, 3) = 243$, respectively. The bit-stream $O_l = “01101100”$ and bit-stream $O_r = “01011101.”$ Consequently, the bit-stream $O = O_l \parallel O_r = “0110110001011101”$. After the pre-processing procedure, the original image shown in FIGURE 3(a) is transformed into the corresponding modified cover image as shown in FIGURE 3(b).

19	19	23	23
19	21	200	6
6	253	12	20
21	20	245	20

(a) Original image

19	19	23	23
19	21	200	12
6	243	12	20
21	20	243	20

(b) Modified cover image

FIGURE 3. An example of pre-processing procedure

3.2. Embedding procedure. In the embedding procedure, let P stand for the payload to be embedded and $|P|$ be the length of payload P . First, P is divided into $|P|/\lfloor \log_2(S_{\max} + 1) \rfloor$ pieces with $\lfloor \log_2(S_{\max} + 1) \rfloor$ bits, and each secret piece is represented as a digital value in a $(S_{\max} + 1)$ -ary notational system, which denotes secret digit S_d belonging to $[0, S_{\max}]$. Except for the modified cover pixels in the first row and first column, each modified cover pixel is processed in raster-scan order to carry a secret digit in a $(S_{\max} + 1)$ -ary notational system. In the proposed method, the secret digit embedding can be classified into two cases, one of which can embed a secret digit S_d while the other cannot.

Case 1. If $e' = |I'(x, y) - I'_p(x, y)| \leq T_1$, $I'(x, y)$ is located at a smooth area, secret digit S_d can be embedded by Equations (4) through (9):

$$r_1 = I'(x, y) \bmod b_1, \quad (4)$$

$$r_2 = I'(x, y) \bmod b_2, \quad (5)$$

$$b_2 = (S_{\max} + 1) \times b_1, \quad (6)$$

$$r'_2 = S_d \times b_1 + r_1, \quad (7)$$

$$d = r'_2 - r_2, \quad (8)$$

$$\hat{I}(x, y) = I'(x, y) + d, \quad (9)$$

where $I'(x, y)$ is a modified cover pixel at coordinate (x, y) in I' , and $I'_p(x, y)$ is a predictive modified cover pixel at coordinate (x, y) in I' obtained by the MED predictor. The e' is a predictive error between $I'(x, y)$ and $I'_p(x, y)$. The r_1 and r_2 are the remainders of $I'(x, y)$ in different bases b_1 and b_2 of notational systems, respectively. The r'_2 is the modified remainder while the S_d is embedded. The d is a difference value between the r_2 and r'_2 . After a secret digit S_d is embedded, the pixel $I'(x, y)$ is modified into $\hat{I}(x, y)$. In order to reduce the distortion of stego-image, we propose an adjusted method, which is formulated as Equation (10):

$$I''(x, y) = \begin{cases} \hat{I}(x, y) - b_2, & \text{if } d > b_2/2, \\ \hat{I}(x, y) + b_2, & \text{if } d < b_2/2, \\ \hat{I}(x, y), & \text{otherwise,} \end{cases} \quad (10)$$

where $I''(x, y)$ is the adjustment modified cover pixel obtained by Equation (10).

Case 2. If $e' = |I'(x, y) - I'_p(x, y)| > T_1$, then $I'(x, y)$ is located at a complex area. In this case, the modified cover pixel is unable to carry any secret digit in order to avoid serious distortion of the stego-image. The corresponding stego-pixel is derived by Equation (11):

$$I''(x, y) = \begin{cases} I'(x, y) + T_2, & \text{if } I'(x, y) > I'_p(x, y), \\ I'(x, y) - T_2, & \text{otherwise.} \end{cases} \quad (11)$$

After the embedding procedure, the modified cover image is converted into a stego-image I'' . We use the following example to demonstrate how a secret digital S_d can be embedded into a modified pixel in the embedding procedure of the proposed method.

Example 2. FIGURE 4(a) shows a 4×4 modified cover image. Let b_1 be 5 and S_{\max} equal 3. The secret data $S = "11"$ can be transformed into a secret digit $S_d = 3$. $T_1 = \lfloor (5 - 1)/2 \rfloor = 2$ and $T_2 = \lfloor (3 + 1)/2 \rfloor \times 5 + 2 = 12$ are calculated by Equation (3). In FIGURE 4(a), the predicted pixel value $I'_p(x, y) = 19$ is computed using the MED predictor from its neighboring pixels $I'(0, 0)$, $I'(0, 1)$, and $I'(1, 0)$. Since the predicted error $e' = |21 - 19| = 2$ is smaller than $T_1 = 2$, $I'(1, 1)$ belongs to **Case 1**. The r_1 , r_2 , b_2 , and r'_2 are 1, 1, 20, and 16, respectively, and obtained by Equations (4) through (7) due to the calculations $r_1 = (21 \bmod 5) = 1$, $r_2 = (21 \bmod 20) = 1$, $b_2 = (3 + 1) \times 5 = 20$, and $r'_2 = (3 \times 5) + 1 = 16$. The difference value d between r'_2 and r_2 is computed as $d = (16 - 1) = 15$. Then, $I'(1, 1)$ is changed as $\hat{I}(1, 1) = 21 + 15 = 36$. Since $d = 15$ is larger than $5/2$, the $\hat{I}(1, 1)$ is changed to $I''(1, 1) = 16$ by Equation (10), i.e. $I''(1, 1) = 36 - 20 - 16$. The next pixel is $I'(2, 1) = 200$, and its predicted value is $I'_p(2, 1) = 23$. Since the predicted error $e' = |200 - 23| = 177$ is greater than $T_1 = 2$, $I'(2, 1)$ belongs to **Case 2**. Because $I'(2, 1) = 200$ is greater than $I'_p(2, 1) = 23$, $I'(2, 1)$ is changed as $I''(2, 1) = (200 + 12) = 212$ by Equation (11). After the embedding procedure, the modified cover image is transformed into the stego-image, as shown in FIGURE 4(b).

19	19	23	23
19	21	200	12
6	243	12	20
21	20	243	20

(a) Modified cover image

19	19	23	23
19	16	212	12
6	243	12	20
21	20	243	20

(b) Stego-image

FIGURE 4. An example of the embedding procedure

3.3. Extracting and restoring procedure. The extracting and restoring procedure is divided into two phases: extracting embedded data and restoring the cover image. In the first phase, the embedded data (i.e. $O||S$) are extracted from the stego-image, and stego-image is recovered into a modified cover image. In the second phase, the original image is restored completely.

3.3.1. Extracting the embedded data. Scanning all stego-pixels in raster-scan order except for the stego-pixels in the first row and first column, we compute the predicted pixel $I_p''(x, y)$ and the predicted error e'' between $I_p''(x, y)$ and $I''(x, y)$. To extract each embedded secret digit S_d and restore the modified cover pixel $I'(x, y)$, the following two cases are considered:

Case 1. If $e'' = |I''(x, y) - I_p''(x, y)| \leq T_2$, then the secret digit S_d is extracted, and $I'(x, y)$ is restored as follows:

$$r'_2 = I''(x, y) \bmod b_2, \quad (12)$$

$$S_d = \lfloor r'_2 / b_1 \rfloor, \quad (13)$$

$$r_1 = r'_2 \bmod b_1, \quad (14)$$

$$r_p = I_p''(x, y) \bmod b_1, \quad (15)$$

$$d_r = (r_1 - r_p) \bmod b_1, \quad (16)$$

$$I'(x, y) = \begin{cases} I_p''(x, y) + d_r, & \text{if } d_r \leq \lfloor b_1/2 \rfloor, \\ I_p''(x, y) + d_r - b_1, & \text{otherwise,} \end{cases} \quad (17)$$

where d_r is the remainder of the difference value between r_1 and r_p .

Case 2. $e'' = |I''(x, y) - I_p''(x, y)| > T_2$, then $I'(x, y)$ is restored as

$$I'(x, y) = \begin{cases} I_p''(x, y) - T_2, & \text{if } I''(x, y) > I_p''(x, y), \\ I_p''(x, y) + T_2, & \text{otherwise.} \end{cases} \quad (18)$$

After all secret data are extracted, the stego-image is recovered into a modified cover image. Example 3 illustrates how to extract a secret digital S_d from the stego-pixel and restore the modified cover pixel.

Example 3. FIGURE 5(a) displays a 4×4 modified image. The pixels located in the first column and row marked in green do not carry any secret data. Assume that $b_1 = 5$ and $S_{\max} = 3$, so that the $b_2 = 20$, $T_1 = 2$, and $T_2 = 12$ can be calculated using Equations (4) through (6). The first pixel to be processed in raster-scan order is $I''(1, 1) = 16$, and its predicted value $I_p''(1, 1) = 19$ can be obtained from $I''(0, 0) = 19$, $I''(0, 1) = 19$ and $I''(1, 0) = 19$ using the MED predictor. The $I''(1, 1)$ belongs to **Case 1**, since the predictive error $e'' = |16 - 19| = 3$ is smaller than $T_2 = 12$. Next, the $r'_2 = 16$ is calculated as $r'_2 = 16 \bmod 20 = 16$, and $S_d = 3$ is extracted by Equation (13) such as $S_d = \lfloor 16/5 \rfloor = 3$. To recover the stego-pixel to the corresponding modified cover pixel, $r_1 = 1$

and $r_p = 4$ are computed according to Equations (14) and (15), i.e., $r_1 = 16 \bmod 5 = 1$ and $r_p = 19 \bmod 5 = 4$. Because of the remainder of difference value between r_1 and r_p , $d_r = (1 - 4) \bmod 5 = 2$ is smaller than $\lfloor 5/2 \rfloor = 2$, so that the $I''(1, 1) = 16$ is modified to $I'(1, 1) = 19 + 2 = 21$ by Equation (17). For the next pixel $I''(2, 1) = 212$, the predicted value $I''_p(2, 1) = 23$ is computed from $I''(1, 0) = 19$, $I''(2, 0) = 23$, and $I'(1, 1) = 21$ using the MED predictor. Since the predicted error $e'' = |212 - 23| = 189$ is greater than $T_2 = 12$, $I''(2, 1)$ belongs to **Case 2**. Hence $I''(2, 1) = 212$ is greater than $I''_p(2, 1) = 23$, so $I''(2, 1) = 212$ is modified to $I'(2, 1) = 212 - 12 = 200$ by Equation (18). After extracting the secret data, the stego-image is restored to the modified cover image as shown in FIGURE 5(b).

19	19	23	23
19	16	212	12
6	243	12	20
21	20	243	20

(a) Stego-image

19	19	23	23
19	21	200	12
6	243	12	20
21	20	243	20

(b) Modified cover image

FIGURE 5. An example of the extracting embedding data phase

3.3.2. Restoring the cover image. After data extracting, each secret digit is transformed into a $\lfloor \log_2(S_{\max} + 1) \rfloor$ -bit code. Therefore, the bit-stream P is generated by concatenating all $\lfloor \log_2(S_{\max} + 1) \rfloor$ -bit codes. For instance, let $S_{\max} = 3$ and the embedded data consist of “12301131032”. The first secret digit “1” is encoded as “01”; the second secret digit “2” is encoded as “10”, and so on. Therefore, the bit-stream P can also be presented as “0110110001011101001110”. However, the front G bits of payload P are code-stream O , and the remainder bits of P are secret data (also called pure payload), where $G = N_o \times k$ and N_o is the number of modified pixel values in $[0, T_2]$ and $[255 - T_2, 255]$. For example, let $T_2 = 12$, $N_o = 4$, $G = 4 \times \lfloor \log_2(12 + 1) \rfloor = 16$. P is “0110110001011101001110”. So that the code-stream O is “0110110001011101” and secret data is “001110”.

Next, the modified cover image can be restored into the original image according to the code-stream O by the following statement:

```

For  $y = 0$  to  $N - 1$ 
  For  $x = 0$  to  $M - 1$ 
    if  $(x = 0$  or  $y = 0)$ 
       $I(x, y) = I'(x, y)$ 
    else if  $(I'(x, y)$  in  $[0, T_2])$  then
       $I(x, y) =$  Take the front  $k$  bits of  $O$  to replace  $k$  least significant bits of  $I'(x, y)$ 
      and then remove the front  $k$  bits from  $O$ ;
    else if  $(I'(x, y)$  in  $[255 - T_2, 255])$  then
       $I(x, y) =$  Take the least  $k$  bits of  $O$  to replace  $k$  least significant bits of  $I'(x, y)$ 
      and then remove the least  $k$  bits from  $O$ ;
    else
       $I(x, y) = I'(x, y)$ 

```

The following serves as a detailed example to describe how the original image can be restored. FIGURE 6(a) shows a 4×4 modified cover image. Let $O = “0110110001011101”$, $b_1 = 5$, $T_2 = 12$, $S_{\max} = 3$, and $k = \lfloor \log_2(12 + 1) \rfloor = 4$. Scanning image in a raster-scan

order, the $I'(3, 1) = 12 = \text{"00001100"}$ is in $[0, 12]$ so that four least significant bits of $I'(3, 1)$ are replaced with the front four bits of code-stream O , i.e. $I'(3, 1) = 12 = \text{"00001100"}$ is replaced with $I(3, 1) = 6 = \text{"00000110"}$. Next, the front four bits of code-stream O are removed such that $O = \text{"110001011101"}$. For $I'(1, 2) = 243 = \text{"11110011"}$, the four least significant bits of $I'(1, 2)$ are changed into the last four bits of code-stream O so that $I'(1, 2) = 243 = \text{"11110011"}$ is modified into $I(1, 2) = 253 = \text{"11111101"}$. Then, the code-stream O becomes "11000101" and so on. The process continues until all bits in the code-stream O are processed. Finally, the original image is reconstructed without distortion as shown in FIGURE 6(b).

19	19	23	23
19	21	200	12
6	243	12	20
21	20	243	20

(a) Modified cover image

19	19	23	23
19	21	200	6
6	253	12	20
21	20	245	20

(b) Original cover image

FIGURE 6. An example of extracting embedding data phase

4. Experimental Results and Analysis. In this section, we investigate the performance of the proposed method. FIGURE 7 displays eleven 512×512 gray-level text images: “Lena”, “Baboon”, “Barbala”, “Boat”, “GoldHill”, “Jet”, “Pepper”, “Sailboat”, “Tiffany”, “Toys”, and “Zelda”. The peak signal-to-noise ratio (PSNR) is adopted to measure the visual image quality between the cover image and stego-image:

$$\text{PSNR} = 10 \log_2(255^2/MSE) \text{ (dB)},$$

$$MSE = \frac{1}{M \times N} \sum_{x=0}^{M-1} \sum_{y=0}^{N-1} (I(x, y) - I''(x, y))^2.$$

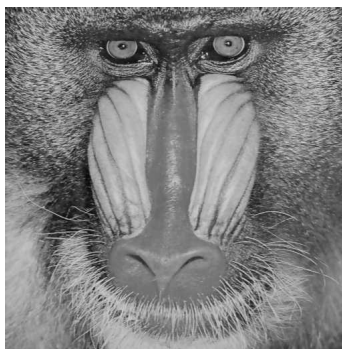
In general, the human eye can hardly distinguish the difference between the original cover image and stego-image when the PSNR value exceeds 30 dB. In this section, pure embedding rate R (also called pure payload) is used to estimate the actual embedding capacity for a method to carry real secret data and is calculated as follows:

$$R = \frac{\text{embedding capacity} - \text{the quantity of overhead data}}{M \times N} \text{ (bpp)}. \quad (19)$$

4.1. The payload and image quality of the proposed method. In the proposed method, the two constants b_1 and S_{\max} determine the embedding capacity and visual image quality. The adjusted embedding capacity and visual image quality make the proposed method flexible and practical for various applications. TABLES 1 and 2 demonstrate the visual image quality measured by PSNR, the amount of overhead information, the embedding capacity (payload) and the pure embedding capacity and pure embedding rate R of the proposed method with various parameters b_1 and S_{\max} for images “Lena” and “Baboon,” respectively. TABLES 1 and 2 indicate that the lower b_1 and S_{\max} provide a higher visual image quality and lower pure embedding capacity, whereas larger b_1 and S_{\max} increase the pure embedding capacity; however, the stego-image undergoes more distortion. To avoid overflow/underflow situations, the proposed method modifies the original pixels when the range of original pixel values fall within $[0, T_2]$ or $[255 - T_2, 255]$. Overhead information is recorded to indicate the original pixel values. From TABLES 1 and 2, only a few overhead information bits (i.e. 4 and 56 bits for “Lena” and “Baboon”,



“Lena”



“Baboon”



“Barbala”



“Boat”



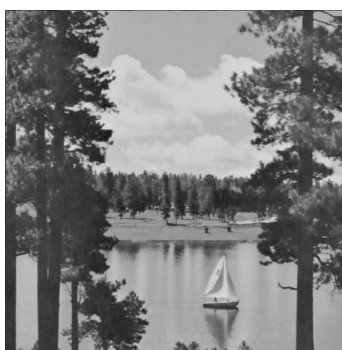
“GoldHill”



“Jet”



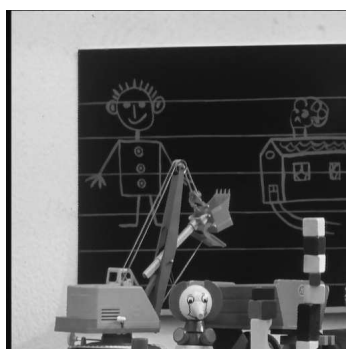
“Pepper”



“Sailboat”



“Tiffany”



“Toys”



“Zelda”

FIGURE 7. The eleven test images

respectively) are recorded when the PSNR value exceeds 30 dB. For the image “Lena”, the maximum pure embedding rate R of the proposed method is about 0.93 bpp, and the PSNR value exceeds 30 dB when the $b_1 = 7$ and $S_{\max} = 2$. For the image “Baboon”, the maximum pure embedding rate R of the proposed method is about 0.37 bpp, and the PSNR value exceeds the 31 dB when $b_1 = 5$ and $S_{\max} = 2$. FIGURE 8 shows the PSNR and pure embedding capacity of eleven test images obtained using the proposed method with different b_1 and S_{\max} .

FIGURE 8 indicates that the proposed method provides better visual image quality (i.e. the average value of PSNR is more than 42 dB when $b_1 = 2$ and $S_{\max} = 1$. When $b_1 = 7$ and $S_{\max} = 2$, the pure embedding rate of the proposed method is more than 1 bpp, and the PSNR of stego-image is over 30 dB for smooth images such as “Lena”, “Boat”, “Jet”, “Pepper”, “Tiffany”, “Toys”, and “Zelda.” However, for complex images such as “Baboon”, “Barbala”, “GoldHill”, and “Sailboat”, the proposed method provides a pure embedding rate of more than 0.5 bpp and a PSNR of more than 32 dB when $b_1 = 5$ and $S_{\max} = 2$.

TABLE 1. The PSNR and embedding capacity of “Lena” obtained using the proposed method with different b_1 and S_{\max}

b_1	S_{\max}	PSNR (dB)	Embedding capacity (bits)	Overhead information (bits)	Pure embedding capacity (bits)	R (bpp)
2	1	42.38	29624	0	29624	0.11
3	1	37.15	77834	0	77834	0.3
3	2	37	123364	0	123364	0.47
4	1	34.15	77834	0	77834	0.3
4	2	34.98	123364	0	123364	0.47
4	3	30.08	155668	0	155668	0.59
5	1	33.06	119447	0	119447	0.46
5	2	32.81	189319	0	189319	0.72
5	3	28.36	238896	8	238888	0.91
5	4	28.1	277350	8	277342	1.06
6	1	31.82	119447	0	119447	0.46
6	2	31.55	189319	0	189319	0.72
6	3	26.97	238896	16	238880	0.91
6	4	26.71	277350	16	277334	1.06
7	1	30.69	153342	4	153338	0.58
7	2	30.33	243041	4	243037	0.93
7	3	26.04	306682	25	306657	1.17
7	4	25.67	356047	25	356022	1.36
8	1	29.77	153342	8	153334	0.58
8	2	29.4	243041	8	243033	0.93
8	3	25.02	306682	25	306657	1.17
8	4	24.62	356047	25	356022	1.36

FIGURE 9 shows that the average maximum PSNR value of the proposed method is 42.374 dB, and the average pure embedding rate R is approximately 0.11 bpp when $b_1=2$ and $S_{\max}=1$. FIGURE 10 shows the PSNR value and the pure embedding rate R of the test images using the proposed method. For the smooth images “Lena,” “Boat,” “Jet,”

TABLE 2. The PSNR and embedding capacity of “Baboon” obtained using the proposed method with different b_1 and S_{\max}

b_1	S_{\max}	PSNR (dB)	Embedding capacity (bits)	Overhead information (bits)	Pure embedding capacity (bits)	R (bpp)
2	1	42.25	15075	0	15075	0.06
3	1	36.6	38974	0	38974	0.15
3	2	36.53	61772	0	61772	0.24
4	1	34.63	38974	3	38971	0.15
4	2	34.56	61772	3	61769	0.24
4	3	29.54	77960	84	77876	0.3
5	1	32.08	61373	21	61352	0.23
5	2	31.98	97274	21	97253	0.37
5	3	27.39	122766	244	122522	0.47
5	4	27.29	142527	244	142283	0.54
6	1	30.89	61375	56	61319	0.23
6	2	30.77	97277	56	97221	0.37
6	3	26.04	122792	424	122368	0.47
6	4	25.92	142557	424	142133	0.54
7	1	29.32	81733	128	81605	0.31
7	2	29.17	129544	128	129416	0.49
7	3	24.7	163564	1185	162379	0.62
7	4	24.55	189892	1185	188707	0.72
8	1	28.45	81735	184	81551	0.31
8	2	28.3	129547	184	129363	0.49
8	3	23.71	163640	1845	161795	0.62
8	4	23.55	189980	1845	188135	0.72

“Pepper,” “Tiffany,” “Toys,” and “Zelda,” the proposed method provides an average value of R up to 1.03 bpp, and the PSNR value is over 30 dB with $b_1 = 7$ and $S_{\max} = 2$. However, for complex images such as “Baboon”, “Barbala”, “GoldHill”, and “Sailboat”, the MED predictor does not precisely estimate the pixel values, so the predicted errors of the most pixels are greater than T_1 , which makes the pixel unembeddable. Therefore, the proposed method offers some pure embedding capacity (i.e. the average value of R is approximately 0.5 bpp) and satisfactory quality of the stego-image (i.e. the average value of PSNR is about 32.27 dB) for complex images when $b_1 = 5$, $S_{\max} = 2$. As shown in the experimental results, the proposed method is more suitably used to embed the secret data in the smooth images.

4.2. Comparison with related methods. For single-layer embedding, the proposed method is compared with difference expansion-based [6, 13], histogram-based [5, 11, 12], and prediction-based [14, 15, 16] reversible image hiding methods for three 512×512 gray-level test images: “Lena”, “Baboon”, and “Jet”. FIGURES 11 through 13 show the pure embedding rates and PSNRs of three test images obtained using difference expansion-based [6, 13], histogram-based [5, 11, 12], prediction-based [14, 15, 16], and proposed methods, respectively. FIGURE 11 indicates that Kim et al.’s [6] method provides better visual image quality than Tian’s method [13] and the proposed method. The pure embedding rate of the difference expansion-based methods [6, 13] is quite limited, whereas the

proposed method obtains a higher pure embedding rate than the difference expansion-based methods. FIGURE 12 illustrates that the histogram-based and proposed methods can achieve a pure embedding rate of about 0.9 bpp (i.e. except for the complex image “Baboon”), but their PSNR values are lower than the difference expansion-based methods. Moreover, for the image “Jet”, the proposed method yields a higher pure embedding rate (R is about 1.2 bpp). From the results shown in FIGURE 13, Thodi et al.’s method achieves a higher pure embedding rate and good visual image quality, except for the image “Baboon”. Tsai et al.’s method obtains a PSNR value of about 50 dB, but its pure embedding rate is very low. The experimental result of the image “Baboon” of Tsai et al.’s method is not presented in FIGURE 13, since the overhead information of Tsai et al.’s method exceeds the maximum embedding capacity. Tseng et al.’s method provides the advantage of free location map, but only has a low embedding rate. The results of the method by Tseng et al.’s show that the relationship between image quality and embedding capacity is irregular so that it is difficult to control the performance. As the results from FIGURE 13, the proposed method can obtain a higher pure embedding rate and a more pleasing PSNR value than other prediction-based methods.

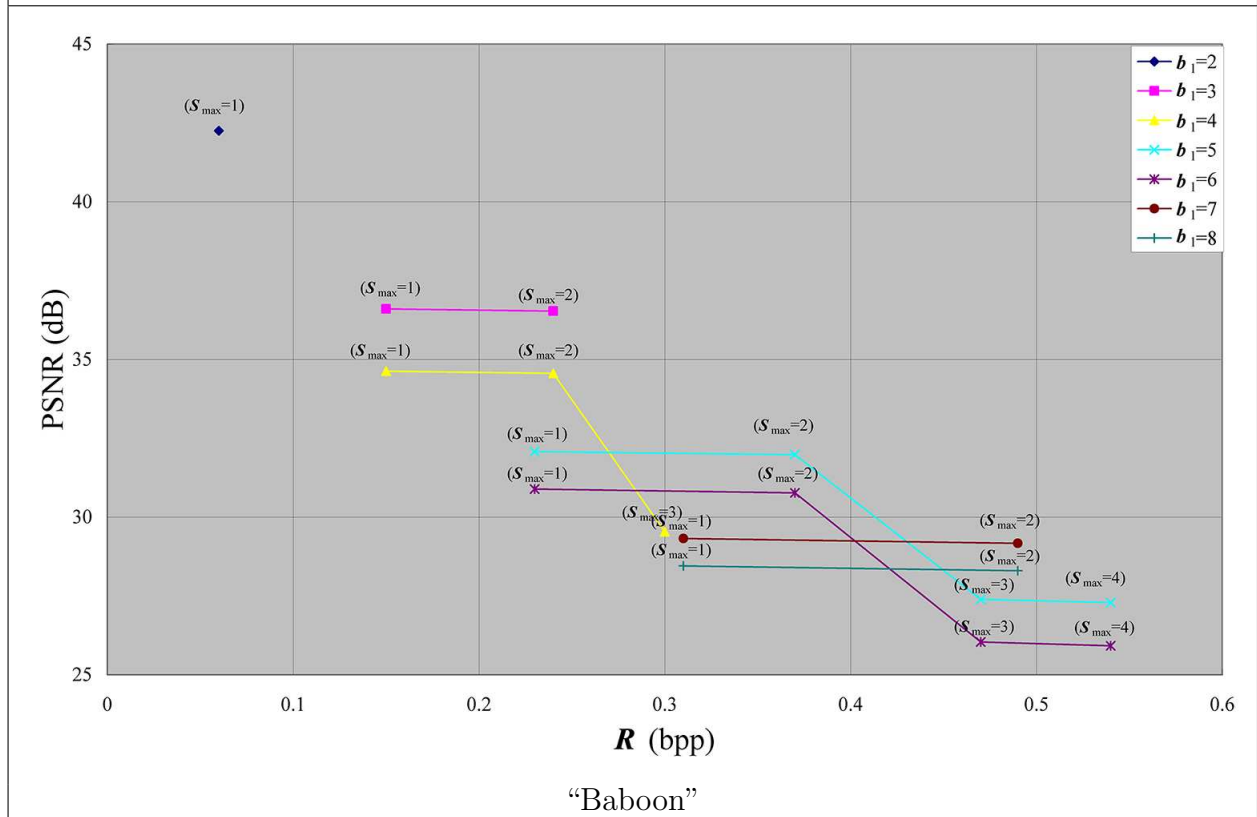
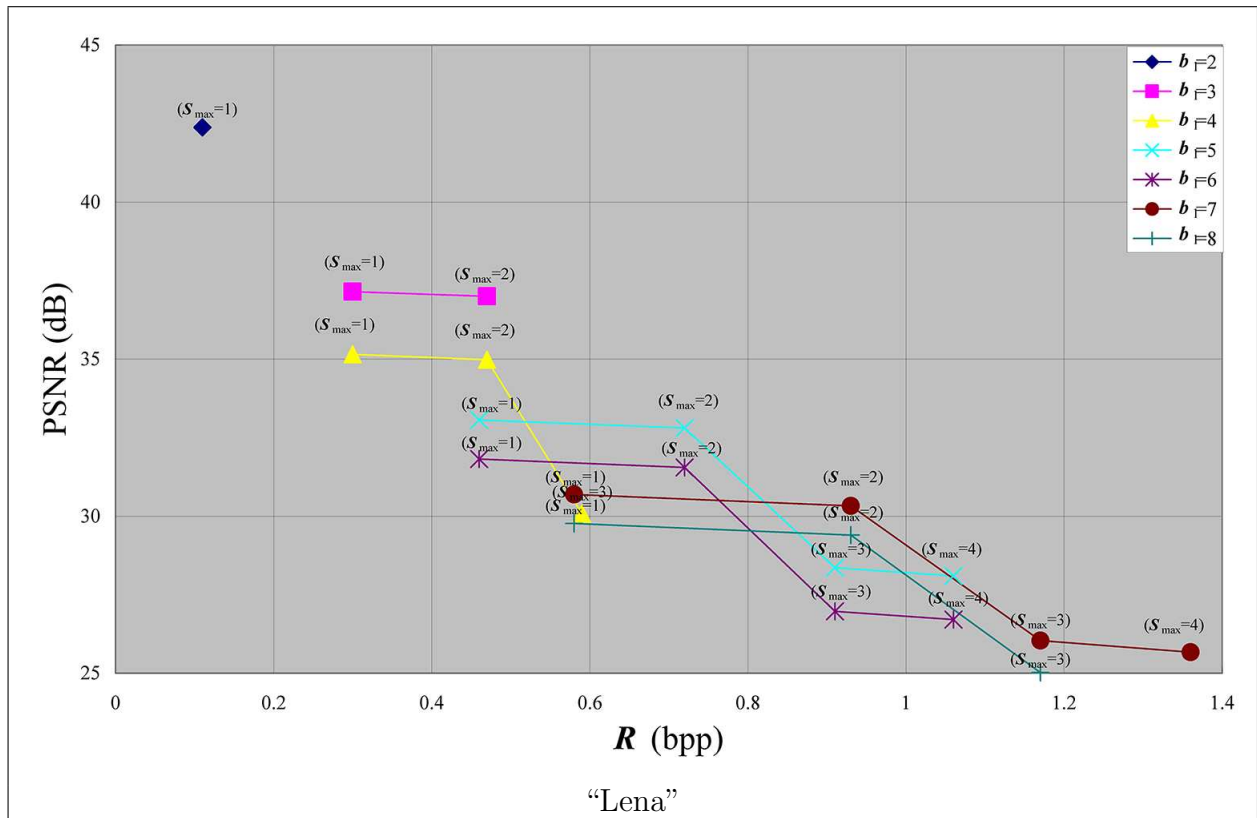
5. Conclusions. In this paper, a novel reversible image hiding method is proposed that exploits the multiple-base notational systems to embed secret data into a cover image with minimal distortion and to achieve a higher pure embedding capacity. In the proposed method, the receiver can completely restore the original cover image from the stego-image without the requirement of a location map while the secret data are extracted. Furthermore, the flexibility of this scheme is that the user can adjust the embedding capacity and the visual image quality by selecting various parameters b_1 and S_{\max} . The experimental results demonstrate that the proposed method provides a high embedding capacity and a stratified visual image quality, especially for smooth images.

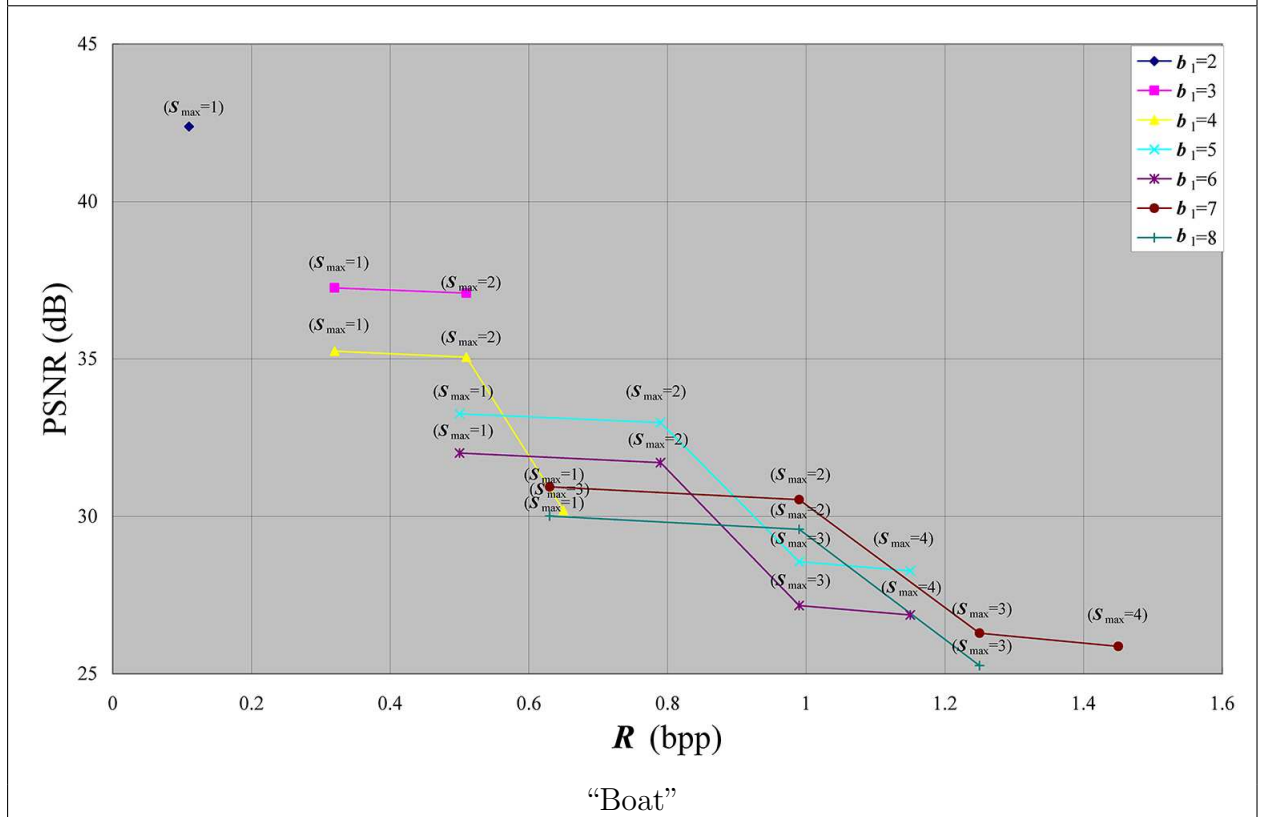
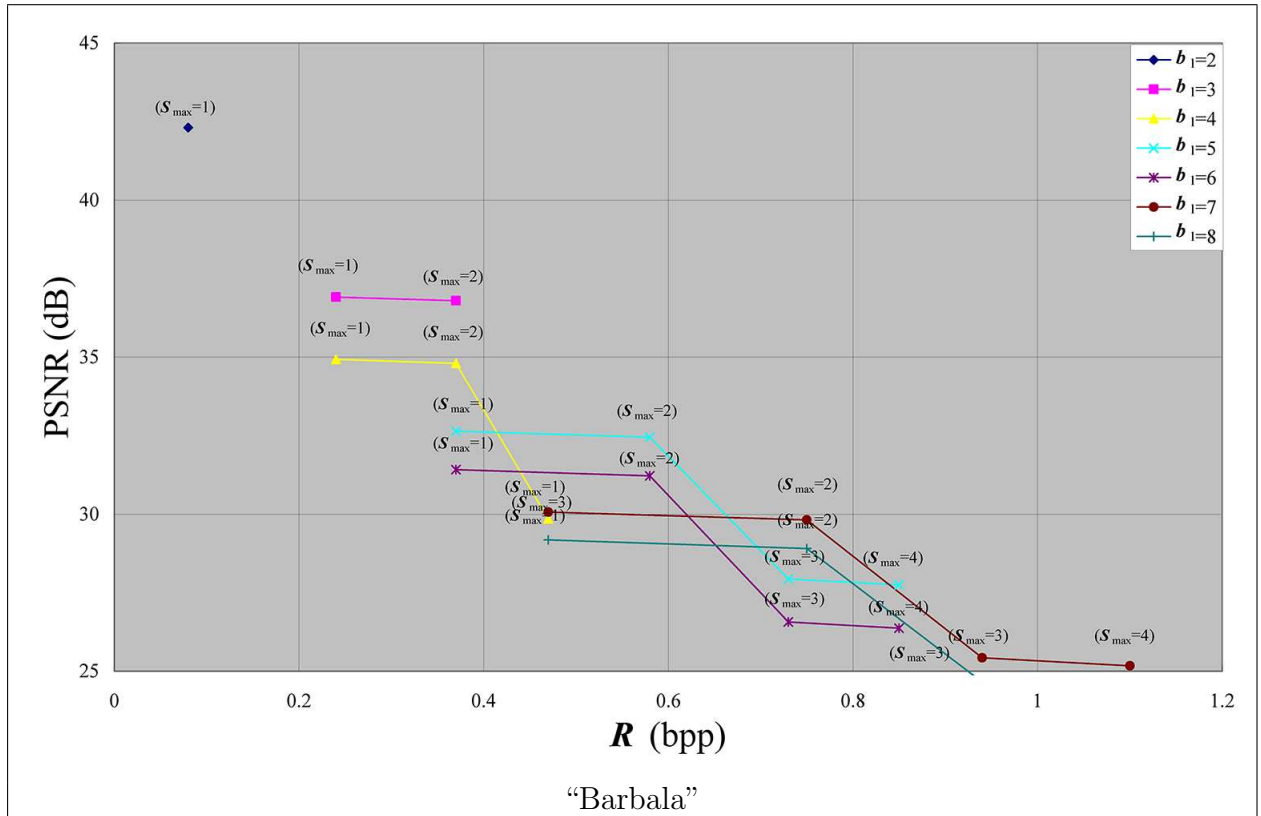
Acknowledgment. This work was supported in part by National Science Council Granted NSC101-2221-E-324-006-MY2.

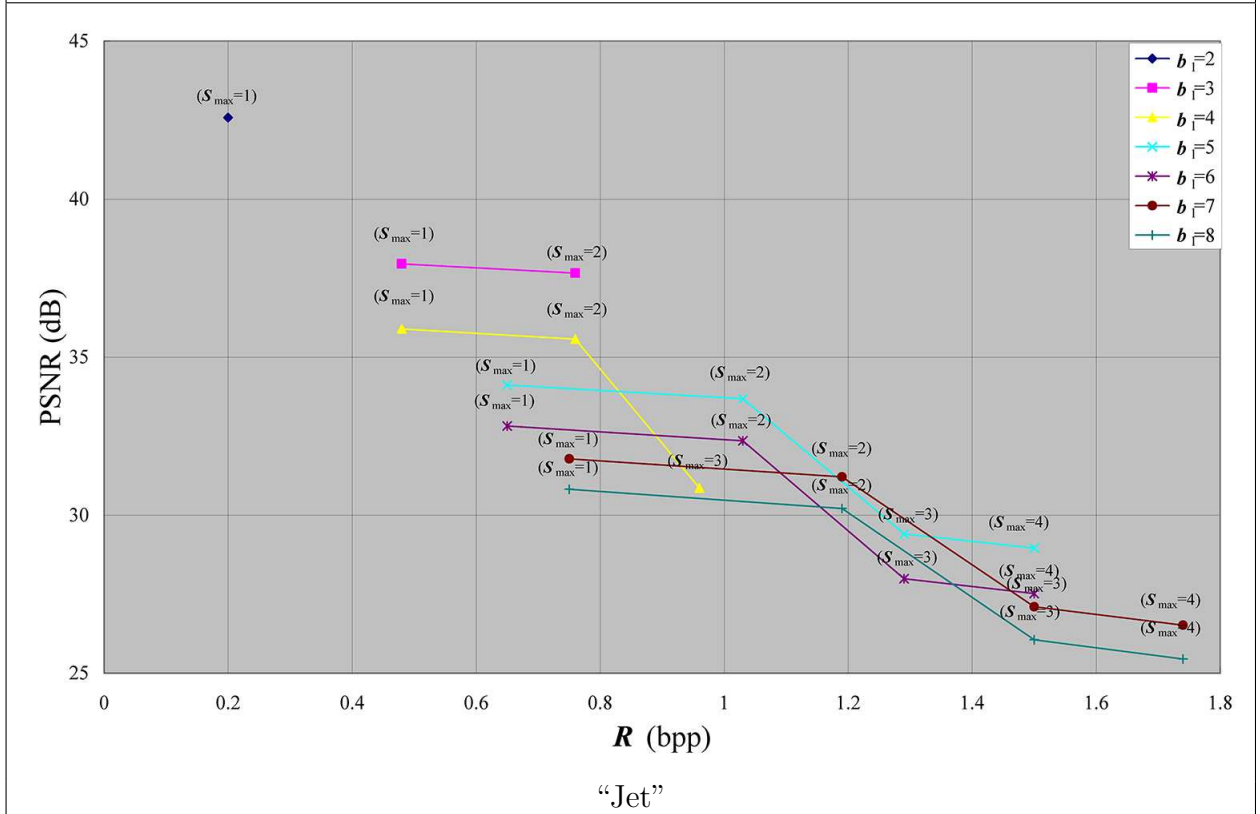
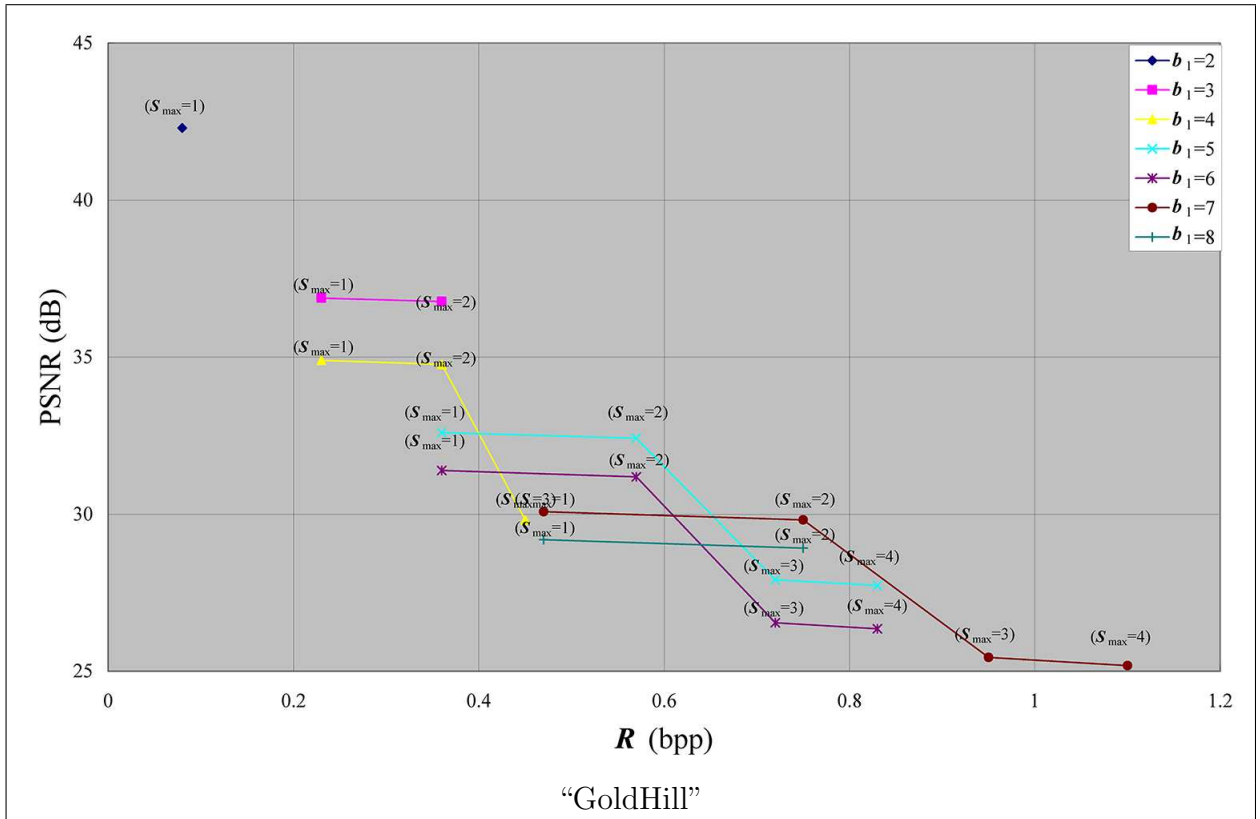
References

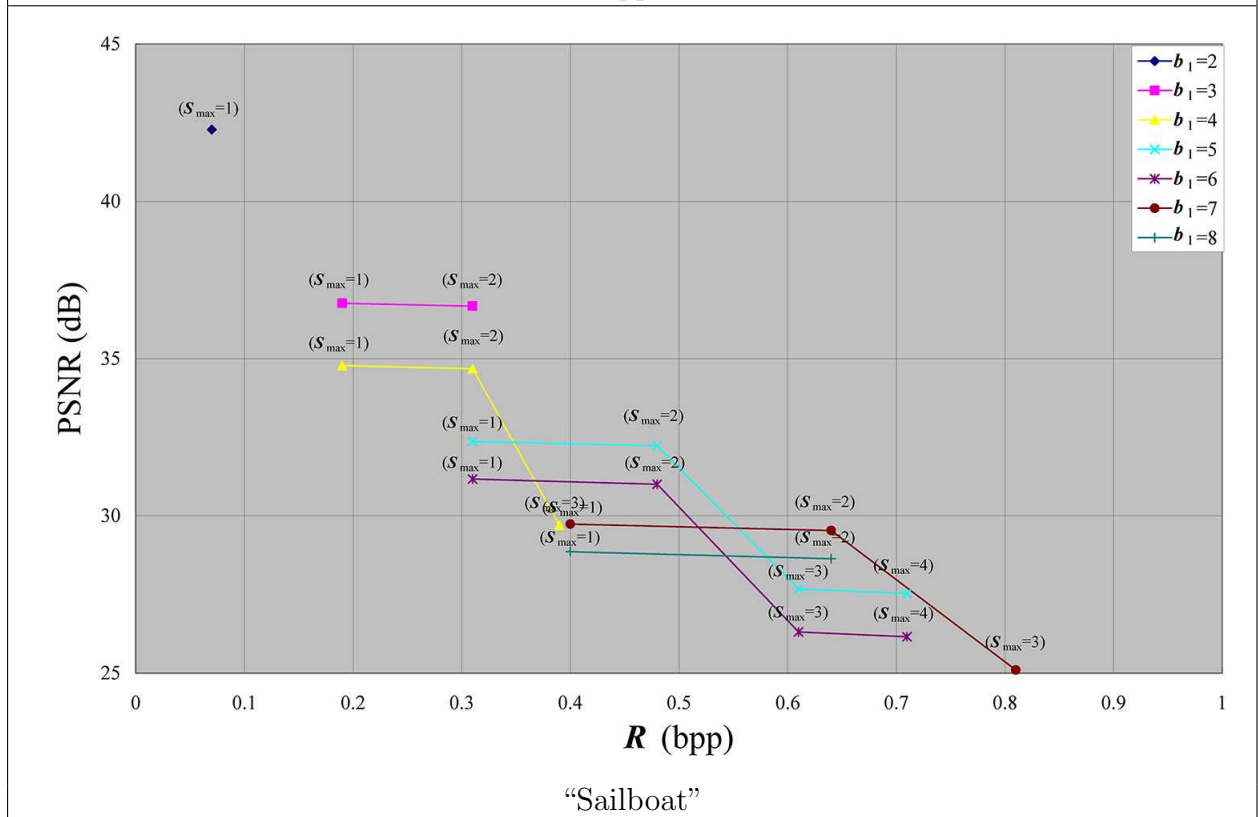
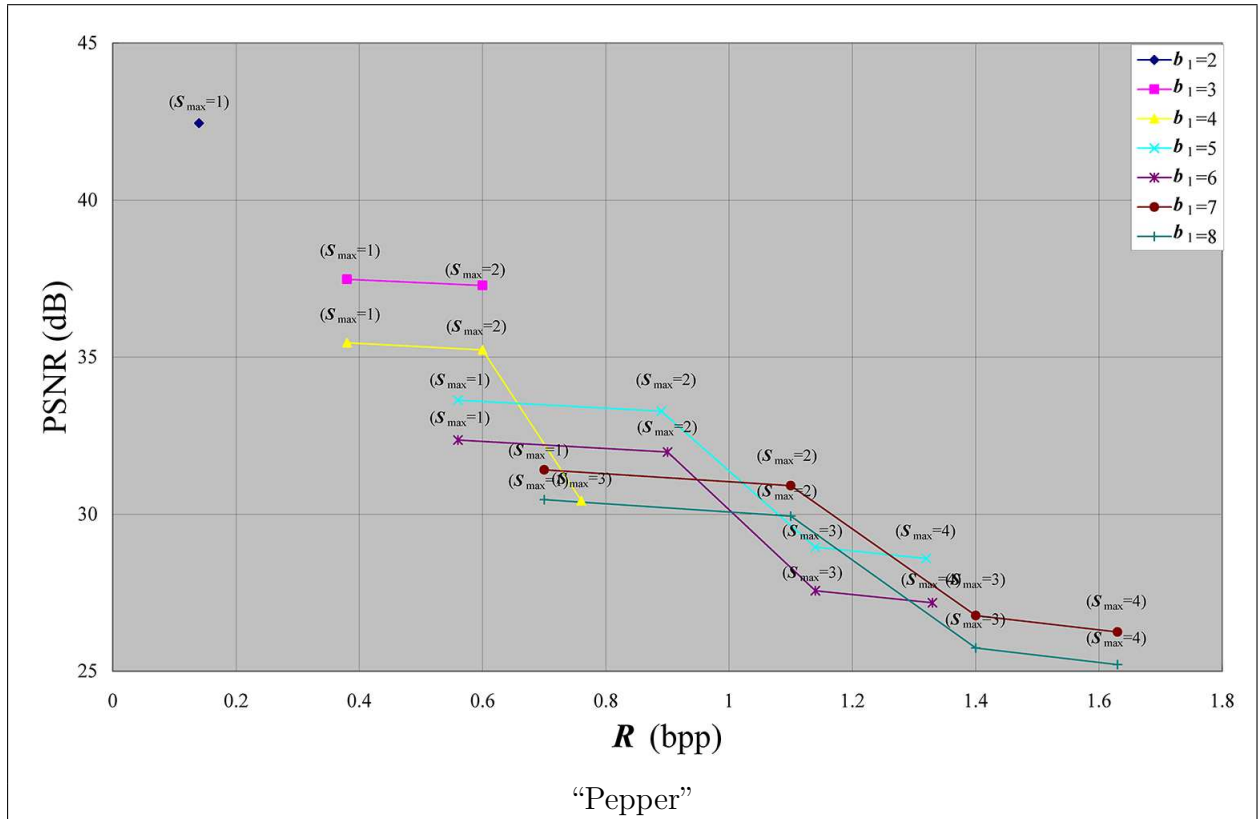
- [1] J. M. Barton, Method and apparatus for embedding authentication information within digital data, *US Patent 5646997*.
- [2] M. U. Celik, G. Sharma, A. M. Tekalp, and E. Saber, Lossless generalized-LSB data hiding embedding, *IEEE Transactions on Image Processing*, vol. 14, no. 2, pp. 253–266, 2005.
- [3] C. De Vleeschouwer, J. F. Delaigle, and B. Macq, Circular interpretation of bijective transformations in lossless watermarking for media asset management, *IEEE Transactions on Multimedia*, vol. 5, no. 1, pp.97–105, 2003.
- [4] J. Fridrich, M. Golijan, and R. Du, Lossless data embedding-new paradigm in digital watermarking, *Journal of Applied Signal Processing*, vol. 2002, no. 2, pp. 185–196, 2002.
- [5] K. S. Kim, M. J. Lee, and H. Y. Lee, Reversible data hiding exploiting spatial correlation between sub-sampled images, *Pattern Recognition*, vol. 42, no. 11, pp. 3083–3096, 2009.
- [6] H. J. Kim, V. Sachnev, Y. Q. Shi, J. Nam, and H. G. Choo, A novel difference expansion transform for reversible data embedding, *IEEE Transactions on Information Forensics and Security*, vol. 3, no. 3, pp.456–465, 2008.
- [7] C. F. Lee, C. C. Chang, and K. H. Wang, An improvement of EMD embedding method for large payloads by pixel segmentation strategy, *Image and Vision Computing*, vol. 26, no. 12, pp. 1670–1676, 2008.
- [8] C. F. Lee, and H. L. Chen, Adjustable prediction-based reversible data hiding, *Digital Signal Processing*, vol. 22, no. 6, pp. 941–953, 2012.
- [9] C. C. Lin, W. L. Tai, and C. C. Chang, Multilevel reversible data hiding based on histogram modification of difference images, *Pattern Recognition*, vol. 41, no. 12, pp. 3582–3591, 2008.

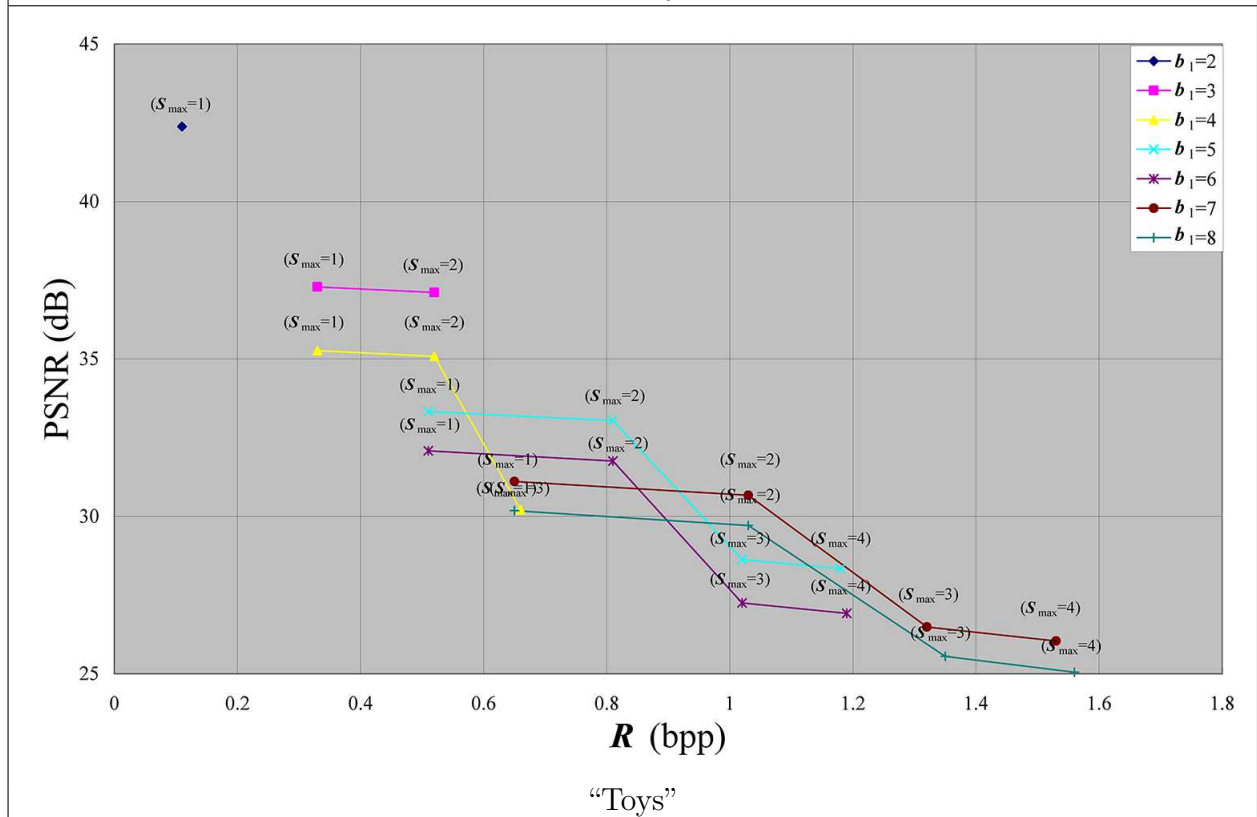
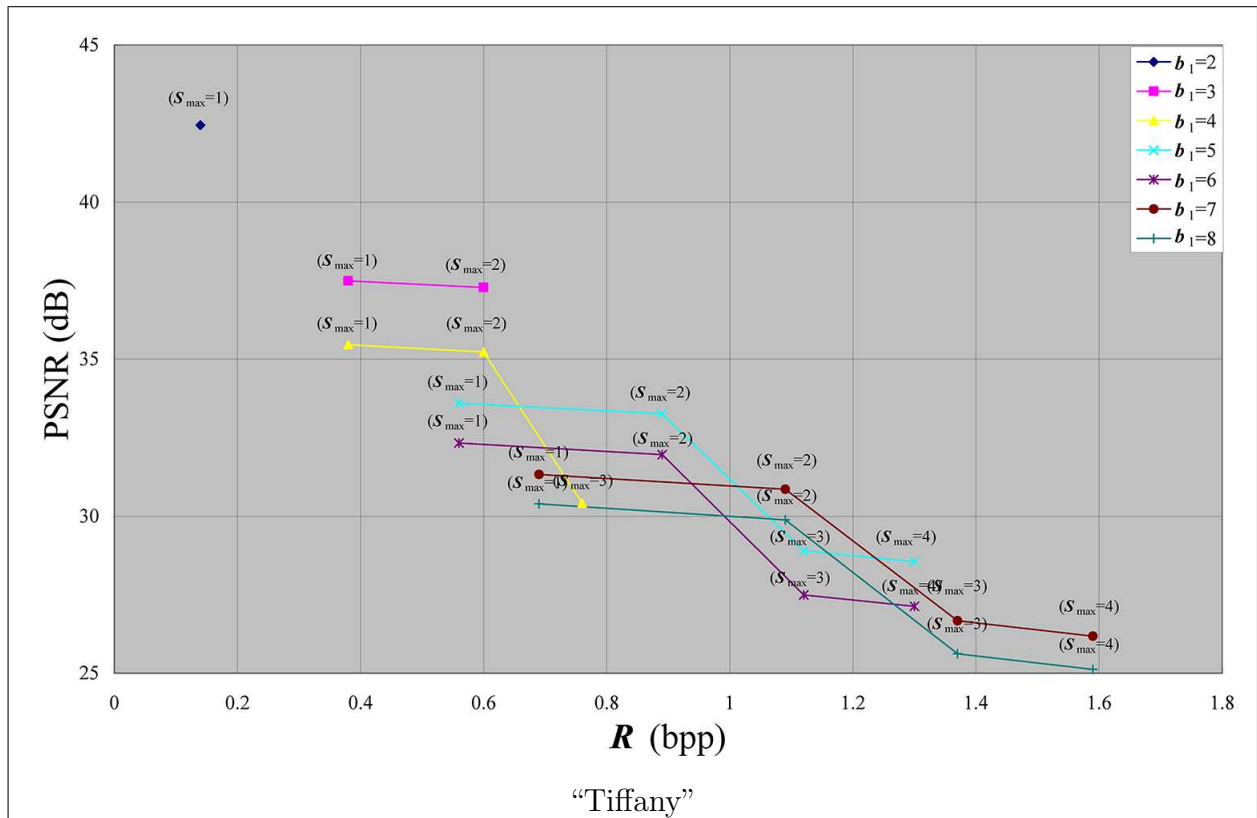
- [10] D. C. Lou, M. C. Hu, and J. L. Lin, Multiple layer data hiding scheme for medical images, *Computer Standards & Interfaces*, vol. 31, no. 2, pp. 329–335, 2009.
- [11] Z. Ni, Y. Q. Shi, N. Ansari, and W. Su, Reversible data hiding, *IEEE Transactions on Circuits and Systems for Video Technology*, vol. 16, no. 3, pp. 354–362, 2006.
- [12] W. L. Tai, C. M. Yeh, and C. C. Chang, Reversible data hiding based on histogram modification of pixel differences, *IEEE Transactions on Circuits and Systems for Video Technology*, vol. 19, no. 6, pp. 906–910, 2009.
- [13] J. Tian, Reversible data embedding using a difference expansion, *IEEE Transactions on Circuits and Systems for Video Technology*, vol. 13, no. 8, pp. 890–896, 2003.
- [14] D. M. Thodi, and J. J. Rodriguez, Expansion embedding techniques for reversible watermarking, *IEEE Transactions on Image Processing*, vol. 16, no. 3, pp. 721–730, 2007.
- [15] P. Tsai, Y. C. Hu, and H. L. Yen, Reversible image hiding scheme using predictive coding and histogram shifting, *Signal Processing*, vol. 89, no. 6, pp. 1129–1143, 2009.
- [16] H. W. Tseng, and C. P. Hsieh, Prediction-based reversible data hiding, *Information Sciences*, vol. 179, no. 14, pp. 2460–2469, 2009.
- [17] L. F. Turner, Digital data security system, *Patent IPN*, WO 89/08915, 1989.
- [18] M. J. Weinberger, G. Serroussi, and G. Sapiro, The LOCO-I lossless image compression algorithm: Principles and standardization into JPEG-LS, *IEEE Transactions on Image Processing*, vol. 9, no. 8, pp.1309–1324, 2000.
- [19] W. H. Wang, C. F. Lee, and C. Y. Chang, Histogram-shifting-imitated reversible data hiding, *Journal of Systems and Software*, vol. 86, no. 2, pp. 315–323, 2013.
- [20] X. Zhang, and S. Wang, Efficient steganographic embedding by exploiting modification direction, *IEEE Communications Letters*, vol. 10, no. 11, pp. 781–783, 2006.











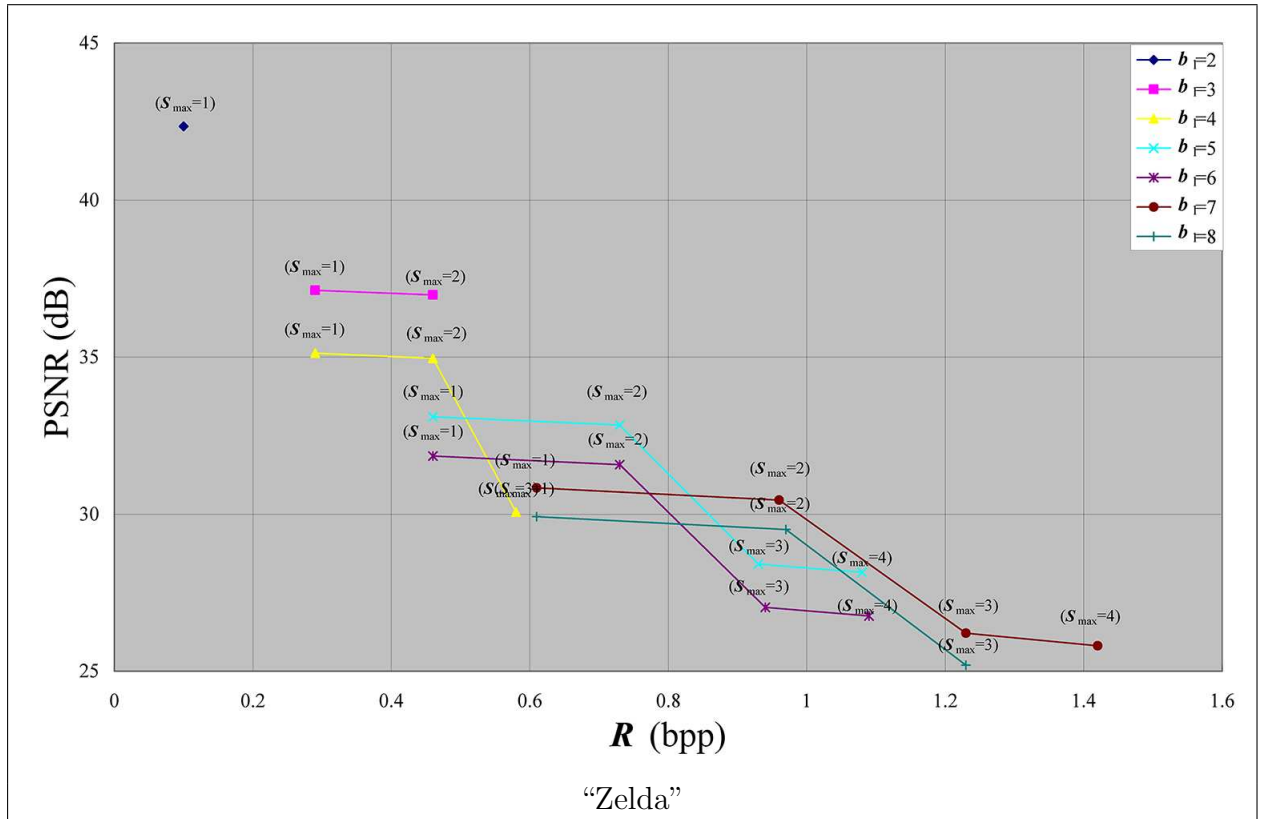

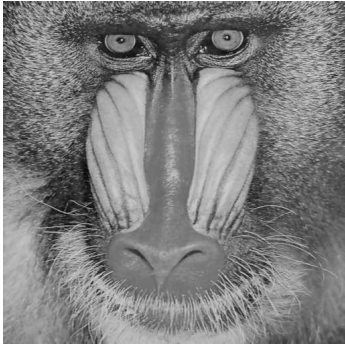









FIGURE 8. The PSNR and pure embedding capacity of eleven test images obtained using the proposed method with different b_1 and S_{\max}

		
“Lena”	“Baboon”	“Barbala”
PSNR = 42.38 dB	PSNR = 42.25 dB	PSNR = 42.31 dB
$R = 0.11$ bpp	$R = 0.06$ bpp	$R = 0.08$ bpp
Pure embedding capacity = 29624 bits	Pure embedding capacity = 15075 bits	Pure embedding capacity = 21514 bits
		
“Boat”	“GoldHill”	“Jet”
PSNR = 42.38 dB	PSNR = 42.30 dB	PSNR = 42.58 dB
$R = 0.11$ bpp	$R = 0.08$ bpp	$R = 0.20$ bpp
Pure embedding capacity = 29387 bits	Pure embedding capacity = 20252 bits	Pure embedding capacity = 51376 bits
		
“Pepper”	“Sailboat”	“Tiffany”
PSNR = 42.45 dB	PSNR = 42.28 dB	PSNR = 42.45 dB
$R = 0.14$ bpp	$R = 0.07$ bpp	$R = 0.14$ bpp
Pure embedding capacity = 36796 bits	Pure embedding capacity = 17581 bits	Pure embedding capacity = 37787 bits

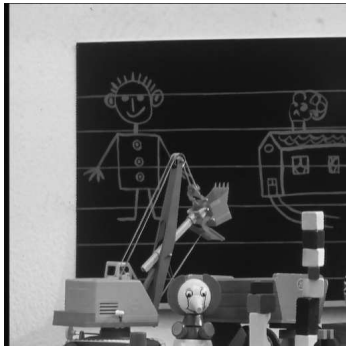


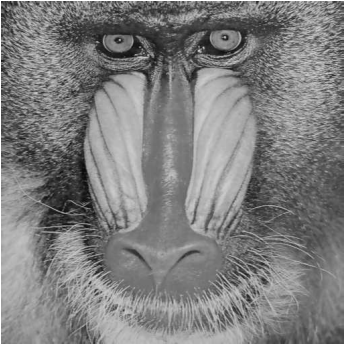







	
“Toys”	“Zelda”
PSNR = 42.38 dB	PSNR = 42.35 dB
$R = 0.11$ bpp	$R = 0.10$ bpp
Pure embedding capacity = 30060 bits	Pure embedding capacity = 25913 bits

FIGURE 9. The PSNR, R , and pure embedding capacity of the test images obtained using proposed method when $b_1 = 2$ and $S_{\max} = 1$

		
“Lena”	“Baboon”	“Barbala”
PSNR = 30.33 dB	PSNR = 31.98 dB	PSNR = 42.45 dB
$R = 0.93$ bpp	$R = 0.37$ bpp	$R = 0.58$ bpp
Pure embedding capacity = 243037 bits	Pure embedding capacity = 97253 bits	Pure embedding capacity = 152034 bits
		
“Boat”	“GoldHill”	“Jet”
PSNR = 30.53 dB	PSNR = 32.42 dB	PSNR = 31.21 dB
$R = 0.99$ bpp	$R = 0.57$ bpp	$R = 1.19$ bpp
Pure embedding capacity = 259788 bits	Pure embedding capacity = 148931 bits	Pure embedding capacity = 310928 bits
		
“Pepper”	“Sailboat”	“Tiffany”
PSNR = 30.91 dB	PSNR = 32.23 dB	PSNR = 30.86 dB
$R = 1.03$ bpp	$R = 0.48$ bpp	$R = 1.09$ bpp
Pure embedding capacity = 270406 bits	Pure embedding capacity = 126816 bits	Pure embedding capacity = 284910 bits

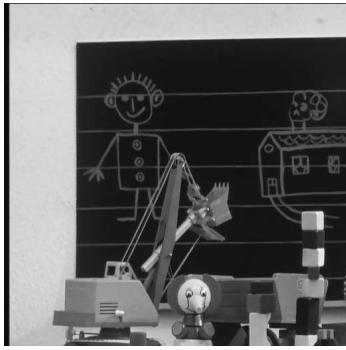

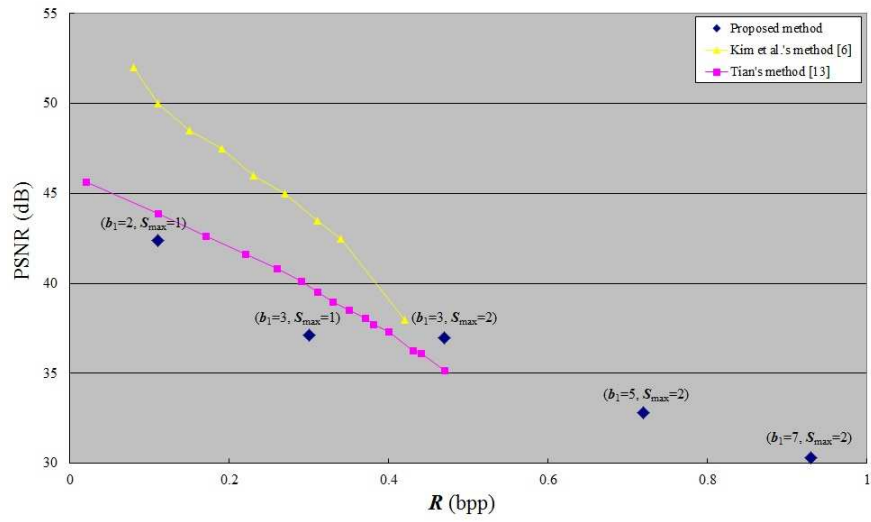
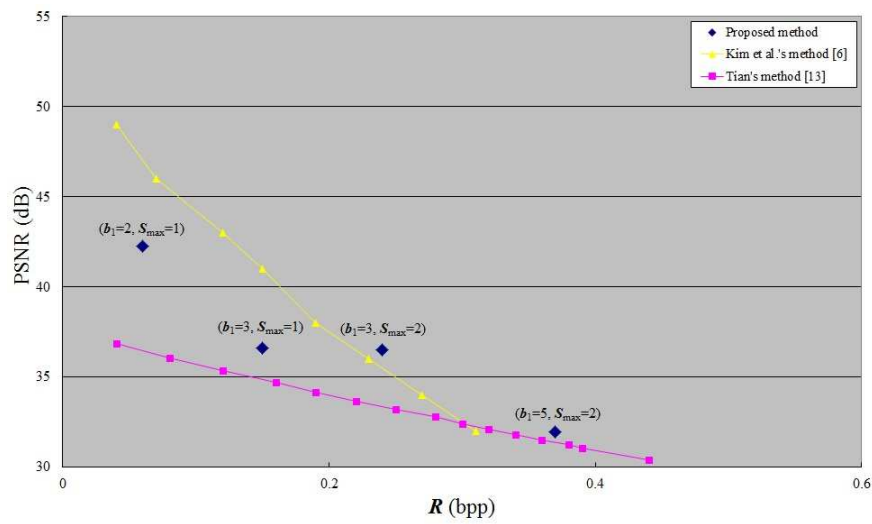
	
“Toys”	“Zelda”
PSNR = 30.67 dB	PSNR = 30.45 dB
$R = 1.03$ bpp	$R = 0.93$ bpp
Pure embedding capacity = 269082 bits	Pure embedding capacity = 244420 bits

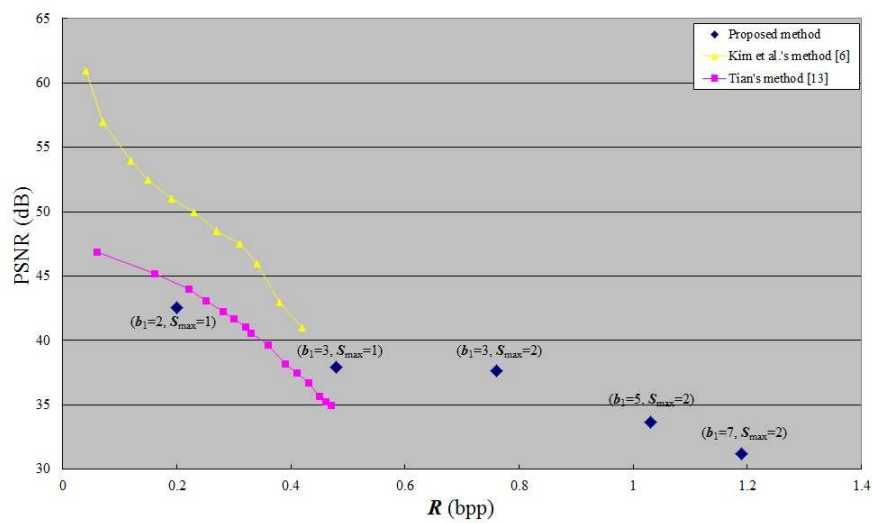
FIGURE 10. The PSNR, R , and pure embedding capacity of the test images obtained using proposed method when $b_1 = 7$ and $S_{\max} = 2$



(a) "Lena"

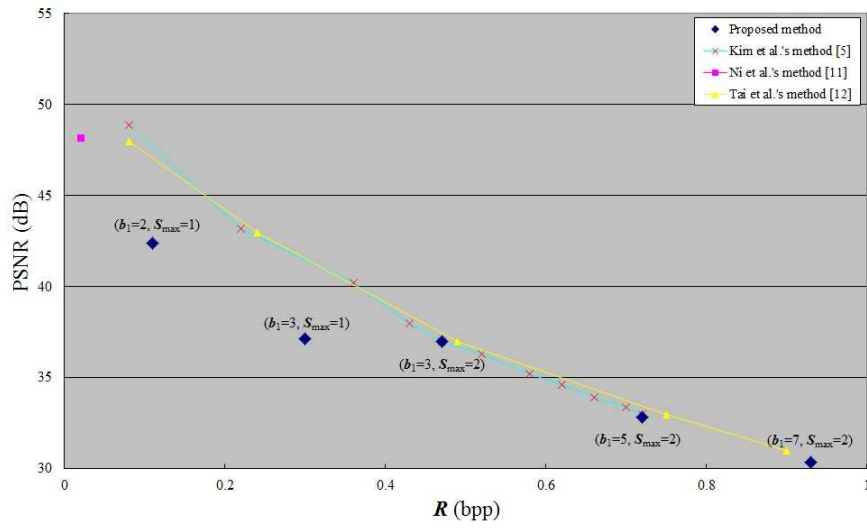


(b) "Baboon"

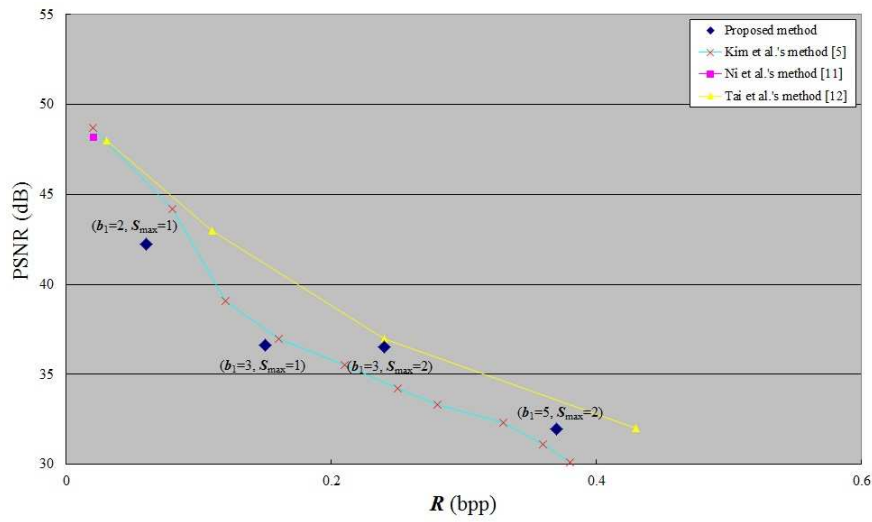


(c) "Jet"

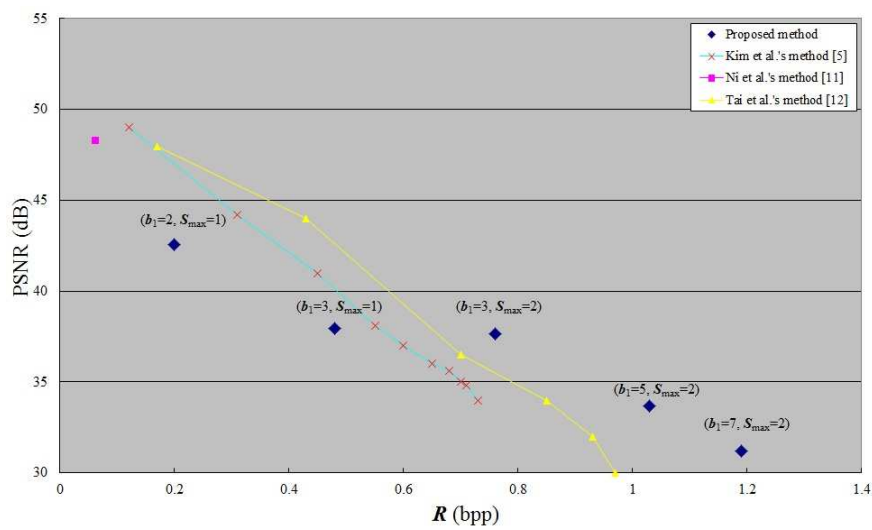
FIGURE 11. The pure embedding capacities and PSNRs of the test images obtained by difference expansion-based and proposed methods



(a) "Lena"

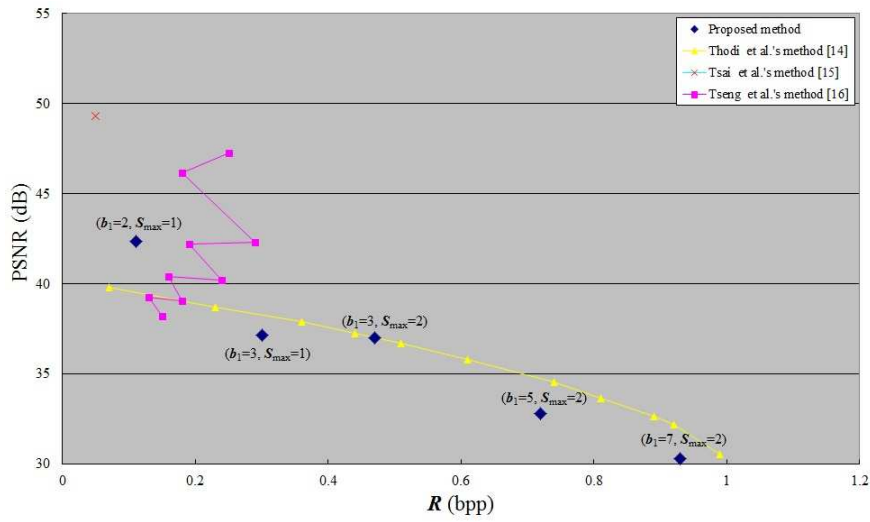


(b) "Baboon"

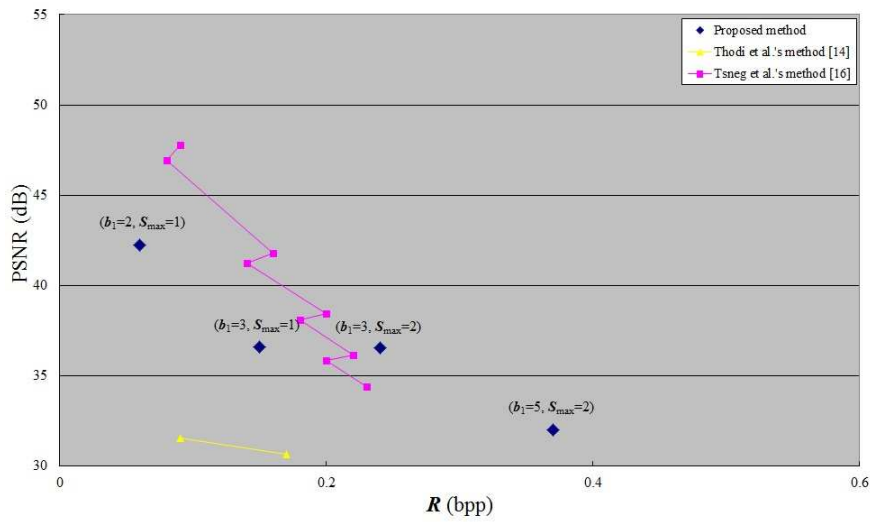


(c) "Jet"

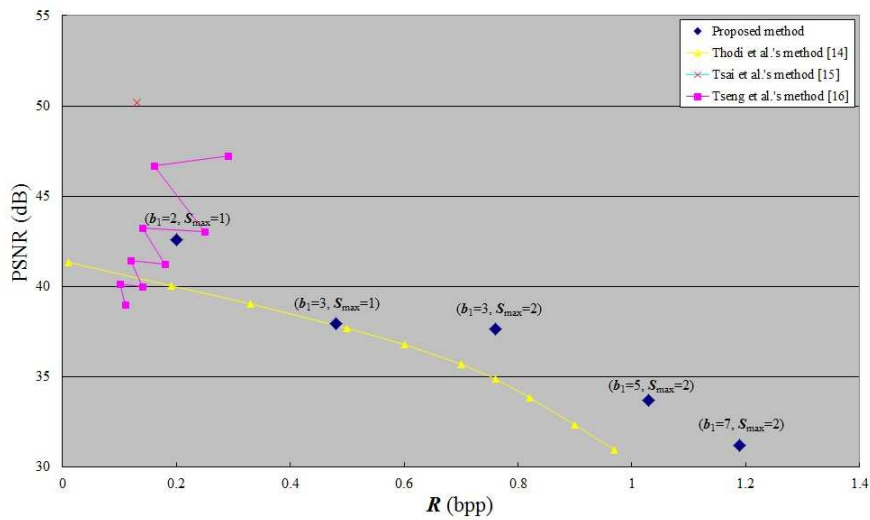
FIGURE 12. The pure embedding rates and PSNRs of the test images obtained by histogram-based, and proposed methods



(a) "Lena"



(b) "Baboon"



(c) "Jet"

FIGURE 13. The pure embedding rates and PSNRs of the test images obtained by prediction-based, and proposed methods